(Reviewer comments in *italics;* Responses in **bold**)

Response to Report#1 Received: 10 Oct 2017

Suggestions for revision or reasons for rejection

General Comments:
Revision: The revision has addressed many concerns and comments, but there are still changes to be made prior to publication.

Detailed comments:

1- Add reference for Goll et al 2012
Response: Included, please check line 725 in marked-up manuscript version.

2- Page 30 line 781-783: Provide a better description of how pools are effected by fire. Arora and Boer do not use the term "penalization fraction", and this term is not clear.
Response: We clarify this in the revised manuscript, please check section 2.2.

3- Page 38 line 985-986: Update sentence to "responsible for altering the simulated AGB to approach the observed AGB". Current sentence structure is unclear.
Response: This has been changed in the revised manuscript. Please check lines 172-180 in marked-up manuscript version.

4- Page 42 line 1092-1094: Update sentence to "showed significant spatial differences".
Response: This has been changed in the revised manuscript. Please check line 461 in marked-up manuscript version.

5- Page 43 line 1109-1112: Update to "vegetation-fire dynamics are mainly controlled"
Response: This sentence has been removed as suggested in Comment 6.

6- Page 43 line 1109-1115: This section needs to be re-written to clearly present how fire effects AGB. Remove the comparison to the work of Hoffman. Arora and Boer clearly describe fire-related mortality with specific reference to tropical burning. Summarize this here. Specifically, does INLAND use the same combustion factors for stem, leaf, and root biomass discussed in Arora and Boer? (To quote Arora and Boer: "The stem wood combustion factor for tropical drought deciduous trees at 0.10 is smaller than that for other PFTs since these trees are characterized by bark that is 3 times thicker than other trees [Hoffmann et al., 2003] which makes them well-adapted for fire-prone savanna regions.")

Response: This has been rewritten in the revised manuscript. The fire occurrence is a disturbance applied equally for all PFTs inside the same pixel. Please check lines 478-488 in marked-up manuscript version.

7- Page 44 line 1179-1183: This should be connected to the above paragraph, or include more discussion. Update to "fire effect implies significant increases" and "resulting in an increase of LAI_{lower}*"*
Response: This has been rewritten in the revised manuscript. Please check lines 485-488 in marked-up manuscript version.

8- Page 44 line 1184: Remove double negative. Update to "model does not include characteristics related to"
Response: This has been changed in the revised manuscript. Please check lines 489-490 in marked-up manuscript version.

9- Page 44 line 1186: Remove double negative. Update to "or the representation of some"
Response: This has been changed in the revised manuscript. Please check line 490 in marked-up manuscript version.

10- Page 45 line 1243: Tree structure would vary temporally rather than spatially. It should be highlighted as an area for improvement, but not in a context of spatial variability.
Response: We agree with the reviewer, this sentence has been modified. Please check line 549 in marked-up manuscript version.

11- Page 48 line 1362: Update to "There is evidence that…"
Response: This has been changed in the revised manuscript. Please check line 635 in marked-up manuscript version.

12- Page 49 line 1370-1371: Update to "With the help of these data, dynamic vegetation models will be able to improve simulation of current…"
Response: This has been changed in the revised manuscript. Please check lines 643-644 in marked-up manuscript version.

Response to Report#2 Received: 10 Oct 2017

All major content-related questions and recommendations have been followed. However, I think that some answers need to be incorporate into the manuscript to improve it. They are:

1- R1Q05 (Referee-1: Question-05)
Response: This was already explained in the first two sentences of Section 2.1.

2- R1Q06 (Referee-1: Questions-06)
Response: This has been included in the revised manuscript. Please check lines 240-247 in marked-up manuscript version.

3- R1Q12 (Referee-1: Question-12)
Response: This has been included in the revised manuscript. Please check lines 577-580 in marked-up manuscript version.

4- R2Q03 (Referee-2: Questions-03)
Response: The discussion was included in Section 4. Please check lines 468-471 in marked-up manuscript version.

5- R2Q04 (Referee-2: Questions-04)
Response: The other PFTs are unaffected. It was already explicit, please check lines 170-171 in marked-up manuscript version.

6- R3Q03 (Referee-3: Questions-03)
Response: This has been included in the revised manuscript. Please check lines 119-120 in marked-up manuscript version.

The answer to the last question from referee #3 should go to the supplementary material.
Response: This has been included in the supplementary material, Section S3.

Influence of climate variability, fire and phosphorus limitation on the vegetation structure and dynamics in the Amazon-Cerrado border

Emily Ane Dionizio da Silva[1], Marcos Heil Costa[1], Andrea Almeida Castanho[2], Gabrielle Ferreira Pires[1], Beatriz Schwantes Marimon[3], Ben Hur Marimon-Junior[3], Eddie Lenza[3], Fernando Martins Pimenta[1], Xiaojuan Yang[4], Atul K. Jain[5]

[1] Department of Agricultural Engineering, Federal University of Viçosa (UFV), Viçosa, MG, Brazil

[2] The Woods Hole Research Center, 149 Woods Hole Rd., Falmouth, MA USA

[3] Federal University of Mato Grosso, Nova Xavantina Campus, Nova Xavantina, MT, Brazil

[4] Oak Ridge National Laboratory, Oak Ridge, TN, USA

[5] Department of Atmospheric Sciences, University of Illinois at Urbana-Champaign

Correspondence to: Emily Ane D. da Silva (emilyy.ane@gmail.com)

Abstract

Climate, fire and soil nutritional limitation are important elements that affect the vegetation dynamics in areas of forest-savanna transition. In this paper, we use the dynamic vegetation model INLAND to evaluate the influence of inter-annual climate variability, fire and phosphorus (P) limitation on the Amazon-Cerrado transitional vegetation structure and dynamics. We assess how each environmental factor affects the net primary production, leaf area index and aboveground biomass (AGB), and compare the AGB simulations of observed AGB map. We used two regional datasets − the 1961-1990average seasonal climate and the 1948 to 2008 inter-annual climate variability, two datasets of total soil P content in soil, based on regional (field measurements) and global data and the INLAND fire module. Our results show that inter-annual climate variability, P limitation and fire occurrence gradually improve simulated vegetation types and these effects are not homogeneous along the latitudinal/longitudinal gradient showing a synergistic effect among them. In terms of magnitude, the effect of fire is stronger, and is the main driver of vegetation changes along the transition. The nutritional limitation, in turn, is stronger than the effect of inter-annual climate variability acting on the transitional ecosystems dynamics. Overall, INLAND typically simulates more than 80% of the AGB variability in the transition zone. However, the AGB in many places is clearly not well simulated, indicating that important soil and physiological factors in the Amazon-Cerrado border, such as lithology and water table depth, carbon allocation strategies and mortality rates, still need to be included in the model.

1 Introduction

The Amazon and Cerrado are the two largest and most important phytogeographical domains in South America. The Amazon forest has been globally recognized and distinguished not only for its exuberance in diversity and species richness, but also for playing an important role in the global climate by regulating water (Bonan, 2008; Pires and Costa, 2013) and heat fluxes (Shukla et al., 1990; Rocha et al., 2004; Roy et al., 2002). The Cerrado is recognized worldwide for being the richest savanna in the world (Myers et al., 2000; Klink and Machado, 2005). It is characterized by different physiognomies, ranging from sparse physiognomies to dense woodland formations, and the latter are commonly mixed with Amazon rainforest forming transitional areas. The Amazon-Cerrado transition extends for 6270 km from northeast to southwest in Brazil, and the ecotonal vegetation around this transition is a mix of the characteristics of the tropical forest and the savanna (Torello-Raventos et al., 2013).

Gradients of seasonal rainfall and water deficit, fire occurrence, herbivory and low fertility of the soil have been reported as the main factors that characterize the transition between forest and savanna globally (Lehmann et al., 2011; Hoffman et al., 2012; Murphy and Bowman, 2012). However, few studies have evaluated the individual and combined effects of these factors on Brazilian ecosystems ecotones (Marimon-Junior and Haridasan, 2005; Elias et al., 2013; Vourtilis et al., 2013).

It is challenging to assess the degree of interaction among these various environmental factors in the transitional region and to infer how each one influences the distribution of the regional vegetation. In this case, Dynamic Global Vegetation Models (DGVMs) can be powerful tools to isolate the influences of climate, fire and nutrients, therefore helping to understand their large-scale effects on vegetation (House et al., 2003; Favier et al., 2004; Hirota et al., 2010; Hoffman et al., 2012).

Previous modelling studies using DGVMs that investigate climate effects in the Amazon indicate that the rainforest could experience changes in rainfall patterns which would either transform the forest into an ecosystem with more sparse vegetation – similar to a savanna, what has been called as the "savannization of the Amazon" (Shukla et al., 1990; Cox et al., 2000; Oyama and Nobre, 2003; Betts et al., 2004; Cox et al., 2004; Salazar et al., 2007) - or to a seasonal forest (Malhi et al., 2009; Pereira et al., 2012; Pires and Costa, 2013). These studies had great importance to the improvement of terrestrial biosphere modeling, but they neglect two important processes in tropical ecosystem dynamics: fire occurrence and nutrient limitation, particularly the Phosphorus (P) limitation.

In tropical ecosystems, fire plays an important ecological role and influences the productivity, the biogeochemical cycles and the dynamics in the transitional biomes, not only by changing the phenology and physiology of plants, but also by modifying the competition among trees and lower canopy plants such as grasses, shrubs and lianas. Fire occurrence, depending on its frequency and intensity, may increase the mortality of trees and transform an undisturbed forest into a disturbed and flammable one (House et al., 2003; Hirota et al., 2010; Hoffmann et al., 2012). Fires also affect the dynamics of nutrients in the savanna ecosystem, changing mainly the N:P relationship and P availability in the soil (Nardoto et al. 2006).

Studies suggest that P is the main limiting nutrient within tropical forests (Malhi et al., 2009; Mercado et al., 2011; Quesada et al., 2012) unlike the temperate forests. Phosphorus is a nutrient that is easily adsorvided by soil minerals due to the large amount of iron and aluminum oxides in the Amazon and Cerrado acidic and strongly weathered soils (Dajoz, 2005; Goedert, 1986). In the tropics, the warm and wet climate favors the high biological activity in the soil and the litter decomposition, not limiting

76 the nitrogen for plant fixation. In Cerrado, higher soil fertility is related to regions with greater woody
77 plants abundance and less grass cover, similarly to the features found in the Amazon rainforest (Moreno
78 et al., 2008; Vourtilis et al., 2013; Veenendaal et al., 2015). However, the phosphorus limitation is often
79 neglected by DGVMs. which usually assume unlimited P availability and consider nitrogen as the main
80 limiting nutrient. However, N is not a limiting nutrient for trees in the tropics (Davidson et al. 2004),
81 while P availability affects the trees dynamics.

82 In principle, in transitional forests, where the climate is intermediate between wet and seasonally
83 dry, the heterogeneous structure and phenology make it difficult to represent these forests in models. The
84 Amazon-Cerrado border is the result of the expansion and contraction of the Cerrado into the forest (see
85 Marimon et al., 2006; Morandi et al., 2016), especially in the Mato Grosso state, where extreme events,
86 such as intense droughts, influence the vegetation dynamics (Marimon et al., 2014) and the nutrient
87 (Oliveira et al., 2017) and carbon cycling (Valadão et al., 2016).

88 Currently, no model has demonstrated to be able to accurately simulate the vegetation transition
89 between Amazon and Cerrado. In general the DGVMs simulate evergreen forest along the Amazon-
90 Cerrado border and neglect savanna occurrence (Botta and Foley, 2002; Bond et al., 2005; Salazar et al.,
91 2007; Smith et al., 2014). This difficulty may be due to absence or not well represented disturbances such
92 as fire, nutritional limitation or soil proprieties. Thus, we need a better understanding of the drivers on
93 transitional vegetation to determine the parameters and establish relations between the environmental and
94 transitional vegetation physiognomies.

95 In this paper we use the dynamic vegetation model INLAND (Integrated Model of Land Surface
96 Processes) to evaluate the influence of inter-annual climate variability, fire occurrence and P limitation

in the Amazon-Cerrado transitional vegetation dynamics and structure. We assess how each element affects the net primary production (NPP), leaf area index (LAI) and aboveground biomass (AGB) and compare the model simulated AGB to observed AGB data. The results presented here are important to build models that accurately represent the transition vegetation, and show the need to include the spatial variability of eco-physiological parameters in these areas.

2 Materials and methods

2.1 Study Area

The present study focuses on the Amazon-Cerrado transition (Figure 1). We use the official delimitation of the Brazilian biomes proposed by IBGE (2004), and define five transects along the transition border with 1° × 1° grid size (the terms "transition", "Amazon-Cerrado transition" and "Forest-Savanna transition" are used interchangeably with the same meaning throughout this manuscript).Transects 1 to 4 are established considering approximately 330 km into the Amazon and 330 km into the Cerrado domain, while Transect 5 is 880 km long on the southern Amazon-Cerrado border. The transects are located as follows: Transect 1 (T1, 44°- 50°W; 5°- 7°S), Transect 2 (T2, 46°-51° W; 7°-9S), Transect 3 (T3, 48°-54° W; 9°-11° S), Transect 4 (T4, 49° - 55° W; 11°-13° S), and Transect 5 (T5, 52° - 60° W; 13°-15° S) (Figure 1).

2.2 Description of the INLAND Surface Model

The Integrated Model of Land Surface Processes (INLAND) is the land-surface component of the Brazilian Earth System Model (BESM). INLAND is basically a revision of the IBIS model (Integrated Biosphere Simulator, described by Foley et al., 1996; Kucharik et al., 2000), through assembly and

standardization of different IBIS versions, and improvements in software engineering. We used the version described by Senna et al. (2009) as starting point for INLAND. No changes in tuning were done since that paper, except the addition of the P parameterization, described below. Code is available from http://www.biosfera.dea.ufv.br/en-US/download-inland.

Excluído: available in http://www.biosfera.dea.ufv.br/en-US/download-inland.

The model considers changes in the composition and structure of vegetation in response to the environment and incorporates important aspects of biosphere-atmosphere interactions. The model simulates the exchanges of energy, water, carbon and momentum between soil-vegetation-atmosphere. These processes are organized in a hierarchical framework and operate at different time steps, ranging from 60 minutes to 1 year, coupling ecological, biophysical and physiological processes. The vegetation structure is represented by two layers: upper (arboreal PFTs) and lower (no arboreal PFTs, shrubs and grasses) canopies, and the composition is represented by 12 plant functional types (PFTs) (e.g., tropical broadleaf evergreen trees or C4 grasses, among several others).The photosynthesis and respiration processes are simulated in a mechanistic manner using the Ball-Berry-Farquhar model (details in Foley et al., 1996). The vegetation phenology module simulates the processes such as budding and senescence based on drought phenology scheme for tropical deciduous trees. The dynamic vegetation module computes the following variables yearly for each PFT: gross and net primary productivity (GPP and NPP), changes in AGB pools, simple mortality disturbance processes and resultant LAI, thus allowing vegetation type and cover to change with time. The partitioning of the NPP for each PFT resolves carbon in three AGB pools: leaves, stems and fine roots. The LAI of each PFT is obtained by simply dividing leaf carbon by specific leaf area, which in INLAND is considered fixed (one value) for each PFT.

INLAND has eight soil layers to simulate the diurnal and seasonal variations of heat and moisture. Each layer is described in terms of soil temperature, volumetric water content and ice content (Foley et al., 1996; Thompson and Pollard, 1995). Furthermore, all of these processes are influenced by soil texture and amount of organic matter within the soil profile.

Considering these aspects of vegetation dynamics and soil physical properties the model can simulate plant competition for light and water between trees, shrubs and grasses through shading and differences in water uptake (Foley et al., 1996). These PFTs can coexist within a grid cell and their annual LAI values indicate the dominant vegetation type within a grid cell. For example, the dominant vegetation type is a Tropical Evergreen Forest if the PFT tropical broadleaf evergreen tree has an annual mean upper canopy LAI (LAI_{upper}) above 2.5 m^2 m^{-2}. On the other hand, the dominant vegetation type is a Tropical Deciduous Forest if the tropical broadleaf drought-deciduous tree has an annual mean LAI_{upper} above 2.5 m^2 m^{-2}. Where total tree LAI (LAI_{upper}) is between 0.8 and 2.5 m^2 m^{-2}, dominant vegetation type is savanna, and LAI_{upper} values smaller than 0.8 m^2 m^{-2} characterize a grassland vegetation type.

We assume that the vegetation types Tropical Evergreen Forest and the Tropical Deciduous Forest in INLAND represents the Amazon rainforest, while Savanna and Grasslands represent the Cerrado. Savanna would be equivalent to the Cerrado physiognomies *Cerradão* and *Cerrado sensu strictu*, while Grasslands would be equivalent to the physiognomies *Campo sujo* and *Campo Limpo* (*sensu* Ribeiro and Walter, 2008).

The soil chemical properties are represented by the carbon, nitrogen and phosphorus. The carbon cycle is simulated through vegetation, litter and soil organic matter, where the biogeochemical module is similar to the CENTURY model (Parton et al., 1993; Verberne et al., 1990). The amount of C existing in

the first meter of soil is divided into different compartments characterized by their residence time, which can vary in an interval of hours for microbial AGB and organic matter to several years for lignin. The model considers only the soil N transformations and carbon decomposition, but the N cycle is not fully simulated and N does not influence the vegetation productivity, i.e., there is a fixed C:N ratio. The P cycle also is not fully implemented, instead the P-limitation is spatially parameterized through the linear relation developed by Castanho et al. (2013) to limit the gross primary productivity. A map of total P available in the soil (P_{total}) is used by the model to estimate the maximum capacity of carboxylation by the Rubisco enzyme (V_{max}) for each grid using Equation (1) :.

$$V_{max} = 0.1013\ P_{total} + 30.037 \qquad (1)$$

where V_{max} and P_{total} are given in $\mu molCO_2\ m^{-2}\ s^{-1}$ and $mg\ kg^{-1}$, respectively. This equation has been based on data for tropical evergreen and deciduous trees, and is applied only to these two PFTs, the other PFTs are unaffected.

INLAND also contains a spatial fire module, based on the Canadian Terrestrial Ecosystem Model CTEM (Arora and Boer, 2005). In this module, three aspects of the fire triangle are considered – the availability of fuel to burn, the flammability of vegetation, and the presence of an ignition source. Each is represented daily by an independently calculated probability and the product of the three is the probability of fire occurrence, calculated daily. Availability of fuel to burn depends on biomass, flammability depends on soil moisture and ignition depends on a random lightning occurrence and a constant anthropogenic ignition probability. The daily fire occurrence probability is equal to the daily AGB burned fraction. The AGB burned fraction is accumulated throughout the year and its ratio is applied at the end of each year to the grid cell area, reducing the leaf, wood and root biomass pools.

Excluído: from

Excluído: (in these runs prescribed to 0.50)

Excluído: The burned area fraction is calculated daily and depends on the probability of ignition, spread rate (as function of wind speed, soil moisture), simulated length to breadth ratio of fire, and extinguishing rate. The daily area burned is accumulated through the year and its ratio to the grid cell area is applied at the end of each year as a "penalization fraction" to leaf, wood and root biomass pools. For more details, see Arora and Boer (2005).

Excluído: aboveground biomass burned fraction is calculated daily and

Formatado: Inglês (Estados Unidos)

Excluído: ly

Formatado: Inglês (Estados Unidos)

Excluído: fire occurrence probability

Excluído:

Excluído: to the grid cell area

Excluído: in

Excluído: Thus the fire occurrence is a disturbance applied equally for all PFTs and does not influencinge the mortality rates.

2.3 Observed data

2.3.1 Phosphorus databases

We used two P databases to estimate V_{max} (Equation 1): one regional (referred to as PR) and one global database referred to as PG). In addition, a control P map (PC) represents the unlimited nutrient availability case, equivalent to a V_{max} of 65 $\mu molCO_2\ m^{-2}\ s^{-1}$, or 350 mg P kg^{-1} soil, according to Equation 1.

The PR database was developed from total P in the soil for the Amazon basin published by Quesada et al. (2011) plus 54 additional available P samples (P extracted via Mehlich-1 extractor, $P_{mehlich-1}$) (Figure 2a). We used the $P_{mehlich-1}$ and clay contents measured in a forest-savanna transition region in Brazil (Mato Grosso state) to estimate P_{total} and expand the coverage area of the P data (Section S1). These 54 samples were gridded to a 1° × 1° grid to be compatible with the spatial resolution used by INLAND, resulting in 12 additional pixels with observed total P content (Figure 2a). For pixels without observed P_{total}, the P_{total} was assumed to be 350 mg P kg^{-1} soil, similarly to the PC conditions.

A global dataset of P_{total} (Figure 2b) was also used to estimate V_{max}. This global data set is part of a database containing six global maps of the different forms of P in the soil (Yang et al., 2013). The P_{total} was estimated from lithologic maps, distribution of soil development stages, fraction of the remaining source material for different stages of weathering using chronosequence studies (29 studies), and P distribution in different forms for each soil type based on the analysis of Hedley fractionation (Yang and Post, 2011), which are part of a worldwide collection of soil profile data. The uncertainties and limitations associated with this database are restricted to the Hedley fractionation data used, which are 17% for low weathered soils, 65% for intermediate soils and 68% for highly weathered soils (Yang et al., 2013).

2.3.2 Above-Ground Biomass (AGB) database

The AGB database used was created by Nogueira et al. (2015) and considered undisturbed (pre-deforestation) vegetation existing in the Brazilian Amazonia. This database was compiled from a vegetation map at a scale of 1:250000 (IBGE, 1992) and AGB averages from 41 published studies that had conducted direct sampling in either forest (2317 plots) or non-forest or contact zones (1830 plots). We bi-linearly interpolated the AGB (dry weight) for each transect considering 1° × 1° to ensure compatibility of the observed and simulated data.

Five longitudinal transects (Figure 1) were individually used to characterize AGB in the Amazon-Cerrado border (Figures 3a and 3b). In T1, T2, T3 and T4, the higher AGB values in the west and lower values in the east are consistent with the transition from a dense and woody vegetation (the Amazon forest) towards a sparse vegetation with lower AGB (the Cerrado). However, T1 shows a more gradual reduction of AGB along the west to east gradient, while in T2, T3 and T4 where the transition is more abrupt. In T5 no west-east gradient is present with high AGB heterogeneity and predominant low AGB across the transect (Figure 3b).

Excluído: separately

2.4 Simulations

The model was forced with the prescribed climate data based on the Climate Research Unit (CRU) database (Harris et al., 2014). Two climate boundary conditions were used: the first is referred to as the monthly climatological average (CA) that represents the average climate for the period 1961-1990. The second climate boundary condition is the historical dataset, for the continuous period between 1948 and 2008, thus considering interannual climate variability (CV). For both boundary conditions, the variables

used are rainfall, solar radiation, wind velocity and maximum and minimum temperatures. The CRU database is developed from observations at meteorological stations across the world's land areas and has been widely used by the scientific community in case studies to evaluate El Niño–Southern Oscillation (ENSO) effects and and other modes of interannual climate variability (Foley et al., 2002; Marengo, 2004; Wang et al., 2014), because these data preserve the spatial mean of the rainfall data, although they do not provide adequate representation of the precipitation variance (Beguería et al., 2016). The dataset has a 1-degree spatial resolution and a monthly time resolution.

Excluído: has

Excluído: reduced rainfall

Excluído: ,

Excluído: ir

Excluído: precipitation

Soil texture data is based on the IGBP-DIS global soil (Global Soil Data Task 2000) (Hansen and Reed, 2000). In the CV group of runs, the model was spin-up by cycling the 1948-2008 climate data (61-year) seven times, totaling 427 years. In the CA group of runs, the annual mean climate data was cycled 427 times. In both cases, CO_2 varied from 278 to 380 ppmv, according to observations in the period, updated annually. In both cases, only the model results of the last 10 years were used to analyze the results.

The experiment design is a factorial combination of the climate scenarios (CA, monthly climatological average, 1961-1990; CV, monthly climate time series, 1948-2008), the nutrient limitation on V_{max} (PC, no P limitation (V_{max} = 65 µmolCO_2 m^{-2} s^{-1}); PR, regional P limitation; PG, global P limitation) and the occurrence of fire (F) or not (Table 1). The 12 combinations in Table 1 allow the evaluation of individual and combined effects of climate, soil chemistry, and the incidence of fire on the variables: Net Primary Production (NPP), tree AGB, and LAI of the upper and lower canopies (LAI_{upper}, LAI_{lower}).

We consider that the subtraction between the simulations (CV+PC) and (CA+PC) represents the isolated effect of inter-annual climate variability without P limitations. The same logic is applied to isolate other factors such as fire and P in different climate scenarios. For example, the fire effect under average climate without P limitation case is calculated by the difference between CA+PC+F and CA+PC. Similarly, the isolated effect of fire under a climate with inter-annual variability scenario without influence of P limitation is calculated by the difference between CV+PC+F and CV+PC. The different combinations of climate scenarios with and without fire effects and with and without P limitations are described in Table 2.

2.5 Statistical analysis and determination of the best model configuration

The statistical analysis is divided in four parts. First, we present maps of the isolated effects for all simulated area calculated as the average of last ten years of simulated spatial patterns. The statistical significance of the isolated effects on NPP, LAI and AGB are determined using the t-test with $p < 0.05$. The results are tested in each pixel, for all the simulated domain (n = 10).

Second, we present an analysis of variance using the one-way ANOVA and the Tukey-Kramer test in the transition zone. We consider all 31 pixels which fall in transects T1 to T5 (n_{pixels}). The results presented are based on the set of last 10 years of simulation (1999-2008, n_{years}) for the 12 combinations ($n_{simulation}$) in Table 1. Moreover, we grouped treatments according to climate regardless of P limitation, presence or absence of fire, where all sets with CV vs CA are tested (Group 1, n=1860, (n_{pixel} x n_{year} x ($n_{simulation}$/2)). Similarly, in Group 2 we tested if PC, PR or PG were significantly different from each other regardless the F or climate used (Group 2, n=1240, (n_{pixel} x n_{year} x ($n_{simulation}$/3)). In Group 3 we tested if fire introduced a significant effect regardless of climate and P limitation (Group 3, n=1860, (n_{pixel} x n_{year}

288 x ($n_{simulation}$/2)). Finally, all treatments were tested to each simulation assessing their individual effects on
289 NPP, LAI and AGB (n_{pixel} x n_{year} = 310).

290 Third, a correlation coefficient between the simulated and observed values for AGB was
291 calculated for each transect. The simulated variables are averaged for the last 10 years of simulations
292 (1999 - 2008) and compared to AGB from Nogueira et al. (2015) within a grid cell.

293 Finally, we evaluate INLAND's ability to assign the dominant vegetation type by analyzing 10
294 years of probability of occurrence. If the dominant vegetation type (evergreen tropical forest, or deciduous
295 forest for the Amazon rainforest, and savanna or grasslands for Cerrado) in a pixel is the same in more
296 than 90% of the simulated years (9 out of 10), then the simulated vegetation type is defined as "very
297 robust" for that pixel; if it occurs in 70 - 90% of the simulated years, the simulated result is considered to
298 be "robust". If the dominant vegetation occurred in less than 70% of simulated years, the pixel is
299 considered "transitional" vegetation.

300 # 3 Results

301 ## 3.1 Influence of climate, fire and phosphorus in the Amazon-Cerrado transition region

302 ### 3.1.1 Spatial patterns

303 Overall, the inclusion of inter-annual climate variability (CV) resulted in a decrease in the
304 simulated average tree biomass (TB) by 3.8% in the entire Brazilian Amazonia, and by 8.7% in the entire
305 Cerrado in comparison to average climate (CA), values obtained by difference CV+PC – CA+PC (Figure
306 4a). The spatial differences between CV and CA for TB simulations are statistically significant and range
307 from -3 kg-C m^{-2} to +2 kg-C m^{-2}. The state of Pará, with higher influence of the El Niño phenomenon,

experienced the highest decrease in TB in the CV simulation. In the state of Roraima, on the other hand, there was an increase of about 2 kg-C m^{-2} in TB when CV was considered. Bolivia and southwest of Mato Grosso state also presented, in some grids points, a significant increase in AGB higher than 2 kg-C m^{-2}.

On average, P acts as a limiting factor in the simulated TB, decreasing by 13% in regional P (PR) simulation and 15% in global P (PG) simulation. In PR, TB decreased mainly in the southeastern Amazonia (between Pará and northeastern Mato Grosso states) and northwestern Amazonas state (Figure 4b). In PG, the largest TB decline occurred in central Amazonia, northeastern Pará and northeastern Mato Grosso (Figure 4c). In Cerrado, on the other hand, TB declined by 2% for PR and 9% for PG with respect to the control simulation. In PR, the few pixels in the Cerrado that have P limitation showed a significant decrease in TB (Figure 4b), while in PG the TB reduction was statistically significant for most of the Cerrado domain, except in southern Tocantins state (Figure 4c).

The tree biomass reduction due to fire events is much higher in magnitude more than due to P limitation or inter-annual climate variability (Figure 4d). The small or null fire effect in the Central Amazon rainforest is related the greater water availability on the Amazonia, which makes the forest naturally not flammable as well as a gradient towards seasonally dryer climate increases the intensity and magnitude of fire effects towards the Cerrado (Figure 4d). The fire effect on TB over the Amazon domain was 21-24% of the P limitation effect (range for PR and PG cases), while the fire effect on TB over the Cerrado was more than 250% of the P limitation effects in CV simulations, which is due to quick growth of grasses after fire occurrence in the latter.

3.1.2 Influence of climate, fire and phosphorus in the transects

Results of the ANOVAs and Tukey-Kramer test indicate that the inclusion of CV, limitation by P (PR and PG) and fire in INLAND led to significantly different averages of NPP, LAI and AGB in the transition zones. This influence of climate, P and fire are shown separately in Tables 3 to Table 5 and combined in Table 6.

The effects of climate and P on productivity show that CV reduces the NPP from 0.68 kg-C m^{-2} yr^{-1} to 0.64 kg-C m^{-2} yr^{-1} (Table 3) and the P effect results in NPP decline from 0.71 kg-C m^{-2} yr^{-1} to 0.64 kg-C m^{-2} yr^{-1} (both PR and PG) (Table 4). The fire effect, moreover, has a positive effect on NPP from 0.66 kg-C m^{-2} yr^{-1} when fire is off to 0.67 kg-C m^{-2} yr^{-1} when fires is on. This difference, albeit low, is statistically significant (Table 5).

In addition CV and P limitation reduce the LAI_{total} in the canopy (Table 3 and Table 4), increasing three times LAI_{lower} and decreasing LAI_{upper} (Table 5). The magnitude of fire effect on AGB (46.7%, Table 5) is greater in relation to the CV (5%, Table 3) and P (14%, Table 4) limitation effects.

Even though CV effects on NPP and AGB for each simulation is not statistically significant, the effects of fire and P limitation (regardless of phosphorus map) are. Fire effects are significant only for structural variables as AGB, LAI_{total}, LAI_{upper} and LAI_{lower}. It presents an increase of LAI total of 1.52 m^2 m^{-2} in CV+PG+F in relation to CV+PG, and of 1.32 m^2 m^{-2} in CV+PR+F in relation to CV+PR (Table 6).

3.1.3 West-East patterns of AGB in the Amazon-Cerrado transition

The model used in this study simulates > 80% of the observed AGB variability in all treatments along the transition area except in T5 (Table 7). It shows that the model is able to capture AGB variability

along the transition area, which is relevant when compared to studies that simulate 50% of the observed AGB variability (Senna et al., 2009; Castanho et al., 2013).

It is not possible to identify a treatment that best represents AGB in all transects (Table 7). A combined analysis of Table 7 and Figure 5 indicates a general agreement that observed AGB decreases from W to E in T1 to T4, and this is well captured by several configurations of the model, with specific differences among them. Overall, CA and PC configurations, being the least disturbed treatments, yield higher AGB, while the introduction of CV, PG and F reduce the AGB. However, the simulated results may be above or below the observed ones, which suggests that additional local factors are not included in the model.

The curves of AGB (Figure 5) show the impact of CV, PG and F along the W-E transition. PG has a high influence on the transition, decreasing the ABG especially in the western part of the transects, where the Amazon vegetation is predominant. This feature is particularly simulated in T3 and T4, where PG decrease the AGB by 2 kg-C m^{-2} in the west pixels of these transects (Figure 5). In T1, T2 and T5, AGB decline is also higher with P limitation when compared to the curves limited only by CV. However, in T1 model simulations tend to underestimate the highest and the lowest AGB extremes, and the absolute values were always underestimated, despite the improvement in correlation with the inclusion of the fire component (Table 7).

In T2, T3 and T4, however, fire changes the simulated AGB, making it closer to the observed AGB in the eastern pixels of the Cerrado domain (Figure 5). In T5 these relations are similar, with climate presenting less influence on AGB decrease than P, and fire appears mainly as an AGB reduction factor.

Excluído: is responsible for altering

Excluído: approach

3.2 Simulated composition of vegetation

Most of the pixels in CA show very robust simulations, with more than 90% of the same vegetation cover in the simulated last 10 years (Figure 6a-c and 6g-i). A larger number of pixels with transitional vegetation were simulated in CV (Figure 6d-f and and 6j-l). An even higher variability in CV compared to CA simulations was observed when we added the effects of P limitation and fire (Figure 6a and 6j-l).

The vegetation composition in all P limitation scenarios for CA simulations resulted in robust simulations for nearly all pixels, except for the north of Cerrado domain (Figures 6a, 6b and 6c). The CA+PC and CA+PR simulations had the same vegetation composition, while CA+PG replaced the deciduous forest by evergreen forest in the central Cerrado region, around 8°S 46°W (Figures 6A, 6B and 6C). This behavior might be related to the higher P_{total} values in PG than PR and PC for the Cerrado region (Figure S1). Cerrado was better represented in CV+PC, CV+PR and CV+PG than in the same CA combinations (Figure 6). The occurrence of forested areas in central Cerrado decreased in CV combinations, these being replaced by the savanna or grassland vegetation class.

When the effect of fire was added to CA simulations, the model simulated an increase in the uncertainty on the vegetation cover classification in the Cerrado region. The effect of fire reduced the presence of deciduous forest in central Cerrado biome as well as in CA+PC, and the vegetation was replaced by evergreen forest in about 5 pixels with clay soils with large water retention capacity in CA+PC+F (Figures 6G, 6H, 6I). In this situation, where there is little water stress in the CA simulation, both evergreen and drought deciduous PFTs have each one very high LAI, and the PFT that dominates can be defined by minor effects. Fire, although active, is probably too small to be relevant in a non-stressed ecosystem. In CV simulations, however, fire effect results in the replacement of the deciduous

and perennial forest by savanna and grasses in all central Cerrado region (Figures 6J, 6K and 6L). These results show the limitations of CA and the importance to consider the interannual climate variability on simulations to improve the vegetation simulated.

For all combinations used, transitional forest areas in the northern and southwestern Cerrado biome are not adequately represented. With >90% of concordance, INLAND assigns the existence of tropical evergreen forest rather than deciduous forest in some pixels in the north of the transition, and the existence of tropical evergreen forest rather than savanna in the southwest, indicating difficulty to simulate transitional vegetation in these regions.

4 Discussion

The inclusion of CV, PR and PG and fire in INLAND showed significant influences on the simulated vegetation structure and dynamics in the Amazon-Cerrado border (Figure 4 and Table 6), suggesting that these factors play key role on vegetation structure in the forest-savanna border and can improve the simulated representation of the current contact zone between these biomes. This is broadly consistent with the literature that investigated causes of savanna existence in the real world (Hoffmann et al., 2012; Dantas et al., 2013; Lehmann et al., 2014). In this study, the spatial analysis and the Tukey-Kramer test (TK) show a difference in magnitude among these factors in vegetation, with fire occurrence and P limitation being stronger than inter-annual climate variability along the transects (Figure 4).

The spatial analysis showed that CV declines AGB predominantly in eastern Amazonia (Figure 4a). Climate of this region is intensely affected by ENSO, which could reduce precipitation by 50%, placing the vegetation under intense water stress (Botta and Foley, 2002; Foley et al. 2002; Marengo et al., 2004; Andreoli et al., 2012; Hilker et al., 2014). This reduction in rainfall in dry years brings in direct

Excluído: El Niño–Southern Oscillation (

Excluído:)

changes in carbon flux (NPP) and stocks in leaves and wood, leading to changes in vegetation structure. In addition to inter-annual changes in the rainfall, inter-annual variability in other climate variables in CV also affect AGB, as average, maximum and minimum temperature, as well as wind speed and specific humidity, and influence photosynthesis on the model both directly (through Collatz and Farquhar equations) and indirectly (e.g. through evapotranspiration). Our results showed significant differences for most part of the biomes, except central Amazonia (Figure 4a), where CV and precipitation seasonality have been pointed as secondary effects on vegetation (Restrepo-Coupe et al., 2013), since there is no shortage of water availability during the dry season.

Along the Cerrado, lower water availability in some years in CV affects tree biomass, although that vegetation is predominantly grassy-herbaceous. The AGB decline is significant for most part of the simulated Cerrado domain (Figure 4a) and average values could represent half the amount of typical tree biomass in this biome. This reduction in AGB reflects INLAND's ability to simulate similar Cerrado conditions and expose the few trees to high water stress.

Throughout the transects, however, no significant difference was found for average AGB between CV+PC and CA+PC by TK at $p<0.05$ (Table 6). On the other hand, when we analyzed the influence of CV for the same pixels, but using all simulations (Table 3), regardless of P limitation and fire occurrences, the results showed that the decrease in AGB by 0.38 kg-C m^{-2} (5.7%) is statistically significant along the transition.

P limitation effect was statistically significant for PR and PG along all the Amazon domain and the main differences between these simulations were the spatial patterns of tree AGB decrease (Figure 4b and Figure 4c). We cannot affirm which of these databases is better because they are the results of

different methodologies and observations (Quesada et al., 2009; Yang et al., 2014). However, PG showed a higher AGB decrease in central Amazonia, northeastern Pará and northeastern Mato Grosso state, indicating that in these areas the P limitation is higher. This result does not corroborate the northwest-southeast AGB gradient found in the Amazon basin, which showed a higher productivity in the west where soils are more fertile than those found in the southeast (Aragão et al., 2009; Saatchi et al., 2007; Nunes et al., 2012; Lee et al., 2013). On the other hand, PR AGB agrees with the northwest-southeast gradient, presenting less limitation in the soils of central Amazonia with declines in AGB mainly in the southeastern part of the rainforest (between Pará and northeastern Mato Grosso states) (Figure 4b).

In Cerrado, P limitation also influenced vegetation (Figure 4c) and presented statistically significant differences when compared CV+PG – CV+PC. In this biome, as well as in the Amazon, tree abundance richness and diversity have been generally associated with increases of soil fertility (Long et al., 2012; Vourtilis et al., 2013), highlighting the importance of P in the composition and maintenance of vegetation, especially in transition areas.

Compared to the Amazon domain, the magnitude of effects of P limitation is lower in the Cerrado. However, few pixels in PR that have P limitation showed a significant decrease in arboreal AGB (Figure 4b), while in PG, we found reduction of AGB for most of the Cerrado domain, except only for the southern Tocantins state (Figure 4c). Despite the differences in spatial patterns, there was no statistically significant differences between PR and PG within the transects (Table 4 and Table 6).

The spatial difference between PG and PR showed that PG is lower than PR in the western Amazonia, and higher in northern Amazonia. Moreover, PG have low P values in south of the transition compared to PR, while in Cerrado domain P values ranged between 120 to 200 mg kg^{-1} (Figure S1).

Although the PR dataset includes every known P data collected in the region, these differences reinforce the need to improve the data of P_{total} in the soils of the Amazon and Cerrado/Amazon transition domains. Currently, P_{total} data in Cerrado is scarce, and make unfeasible to establish a proxy similar to Castanho et al. (2013), which was specific for the Amazon.

In INLAND, the simple P-limitation parameterized through the linear relation Vmax and P_{total}, showed significant spatial differences in AGB simulated and an improvement in simulations, highlighting the importance of P-limitation in modeling studies. For the most part, Dynamic Global Vegetation Models (DGVMs) do not consider the complete phosphorus cycle (see exceptions in Goll et al., 2012 and Yang et al., 2014), despite the importance of nutrient cycling for AGB maintenance and tropical vegetation dynamics in dystrophic soils. For example, nutrient cycling in the Amazon/Cerrado transition is closely related to the hyper-dynamic turnover of the AGB (Valadão et al. 2016), in which some key species might also be crucial to the hyper-cycling of nutrients through which vegetation sustain the constant input of nutrients, including large annual amounts of available P (Oliveira et al. 2017). In addition, there is influence between weather and nutrients: a very intense rain can leach nutrients, such as nitrogen, as well as strong winds can carry clay particles where numerous nutrients are adsorbed. However, in this work the nutritional conditions are prescribed and fixed.

The fire occurrence is an important factor controlling the AGB dynamics in the Cerrado or in the transition vegetation (Hoffman et al.,2003; Hoffman et al., 2012; Silvério et al., 2013; Couto-Santos et al., 2014; Balch et al., 2015), which this study clearly replicates, showing statistically significant influences when compared to control simulations (Figure 4d and Table 5). In the transition, the fire effect may reduce average AGB by 50% (Table 5), which under climate change or deforestation conditions may

Excluído: ly

lead to an even stronger change in the vegetation structure and dynamics. In INLAND, the fire disturbance reduces the biomass of all pools and PFT's by the same fraction inside each pixel at the end of every year. Thus, upper and lower LAI are decreased, according to the fire probability, triggering competition between both canopies for light, and increasing the photosynthesis rates and stocks of carbon in leaves, stems and roots pools in the lower canopy. The carbon allocation and mortality rates in INLAND are fixed parameters for each PFT and are not modified after fire occurrence. Thus, during recovery from a fire, the vegetation dynamics follows the model standard procedure.

The dynamics between the upper and lower canopies and the changes in canopy structure after fire occurrence are exclusively due to the canopy opening and consequently more penetration of photosynthetic radiation into the lower canopy. This competition implies in significant increase on the lower canopy resulting in increment of LAI_{lower} (Table 5).

The model does not include fire characteristics such as velocity, intensity and duration of the burning (Hoffman et al., 2003; Rezende et al., 2005; Elias et al., 2013; Reis et al., 2015) or the representation of some tree morphological adaptation that confers to Cerrado species resilience to fire occurrence, such as bark thickness. Thus, trees and grasses throughout the Amazon-Cerrado border are equally exposed to the same fire intensity inside the grid cell, without fire resistance differences. However, despite the limitations in the representation of resilience characteristics and morphological attributes of fire resistance, our results show that simulated biomass is more close to observed biomass in Cerrado areas when the fire module is activated (Figure 5). An improvement in distribution of biomes along the simulated transition area is also observed (Figure 6g-i), highlighting fire as an essential factor to represent the Amazonia-Cerrado border.

Excluído: According to Hoffmann et al. (2009) the undisturbed forests in the Amazon-Cerrado border appear to be more resilient to fire in relation to the other tropical forests and the vegetation-fire dynamics is mainly controlled by tree "topkill" (defined by the authors as complete death of the aerial biomass).

Excluído: effect of fire

Comentado [E1]: *1-This section needs to be re-written to clearly present how fire effects AGB. Remove the comparison to the work of Hoffman.* ***Arora and Boer clearly describe fire-related mortality with specific reference to tropical burning. Summarize this here.*** *Specifically, does INLAND use the same combustion factors for stem, leaf, and root biomass discussed in Arora and Boer? (To quote Arora and Boer: "The stem wood combustion factor for tropical drought deciduous trees at 0.10 is smaller than that for other PFTs since these trees are characterized by bark that is 3 times thicker than other trees [Hoffmann et al., 2003] which makes them well-adapted for fire-prone savanna regions.")*

Excluído: on

Excluído: AGB

Comentado [E2]: *2-This section needs to be re-written to clearly present how fire effects AGB. Remove the comparison to* ...

Comentado [E3]:

Excluído: is similar to the "topkill" presented by Hoffmann et al ...

Excluído: Therefore,

Formatado: Cor da fonte: Vermelho

Excluído: at the end of every year both

Excluído: amount burned

Excluído: is

Excluído: is

Excluído: , as observed in some species of the savanna-forest ...

Excluído: .

Excluído: ¶ ...

Excluído: increases

Excluído: s

Comentado [E4]: This should be connected to the above ...

Excluído: in shrubs and herbaceous vegetation

Excluído: and decreases in the arboreal component,

Excluído: and decrease of LAI_{upper}

Excluído: These changes in canopy structure after fire occurrenc ...

Excluído: M

Excluído: The m

Excluído: neither

Excluído: related to resilience such

Excluído: n

This study shows an improvement in the correlations between simulated and observed AGB when compared to previous modeling studies, regardless of treatment, with correlation coefficients usually above 0.80 for the transects, except for T5, for which the correlation coefficient value is usually below 0.5 (Table 7). Senna et al. (2009) found 0.20 as maximum correlation coefficient between simulated and observed ABG while Castanho et al. (2013) showed 0.80 for Amazonia domain. From Figure 5, it is clear that CV, F and P limitation in the transition zone reduce the AGB, causing the simulated data to approach the observed data. However, the inclusion of these effects is still insufficient to represent the correct distribution of the vegetation types throughout the Amazon-Cerrado border (Figure 6L). In our interpretation, this means that other important factors are still missing from the simulation, especially in T5, where soils are rocky and shallow. A better spatial representation of soil physical properties, including shallow rocky soils, as well as spatially varying physiological parameterizations of the vegetation such as carbon allocation, deciduousness of vegetation, residence time, are probably needed to improve the simulations, in particular in the northern and southern extremes of the border (T1 and T5).

Excluído: and tree structure that may discern thick from thin trees

In addition, literature shows that in the transition area, soils are very different than Amazon soils, and that essential proprieties for modeling are peculiar (Silva et al., 2006; Vourlitis et al., 2013; Dias et al. 2015). For example, Dias et al. (2015) recently showed that the pedological functions normally used by DGVMs may underestimate the saturated hydraulic conductivity (K_s) by >99%, transforming a well-drained soil with $K_s = 1.5.10^{-4}$ m.s^{-1} (540 mm.h^{-1}) in reality into an impervious brick with $K_s = 3.3.10^{-7}$ m.s^{-1} (1.2 mm.h^{-1}) in the model.

For all transects, the AGB curves have similar patterns (Figure 5); the smaller difference is observed between CA+PC and CV+PG curves, while the larger difference is when fire is present. The

effect of P limitation appears as an effect of intermediate magnitude, reducing the AGB by more than the effect of inter-annual climate variability. In the east, it is observed that there is little or no difference among AGB simulated by CA+PC, CV+PC and CV+PG, revealing that inter-annual climate variability and P have smaller influence in the AGB. However, in the east of T2, T3 and T4, fire is the factor that adjusts the simulated to the observed data (Figure 5), differently than the grid points in the West, where CV+PG is a better proxy between observed and simulated data.

Such conditions are interesting because they reflect the different mechanisms that regulate the structure of these ecosystems and probably the phytophysiognomies distribution. For example, P limitation seems to be the factor that improves simulated AGB in regions where the predominant vegetation type is the tropical rainforest. Fire, on the other hand, improves the AGB in grid points where the Cerrado occurs. Moreover, important factors such as productivity partitioning into leaves, roots and wood carbon pools are assumed to be fixed in space and time within a given PFT, neglecting the natural capacity of transitional forests to adapt itself and to adjust their metabolism to local environmental conditions (Senna et al., 2009). In years of severe drought, or under frequent fire occurrence, transitional forests could prioritize the stock of carbon in fine roots instead of the basal or leaf increment to maximize access to available water, make hydraulic redistribution of soil moisture to maintain the greenness and photosynthesis rates, or increase the capacity to resprout after fire occurrence (Hoffman et al., 2003; Brando et al., 2008). Brando et al. (2008) found changes in carbon allocation after an artificial drought in eastern Amazonia, with wood production reduced by 13-60%, and associated increase in root production. Although in INLAND low soil moisture can reduce the photosynthetic rates, carbon allocation rates are fixed (Figure 5a).

Excluído: high sensitivity

Excluído: for

Excluído: basin trees

Excluído: which

Excluído: reduced

Excluído: in response to an artificial drought

Excluído: during the months of lower rainfall

Excluído: it does not dynamically change the

Excluído: , exposing the PFTs in these areas to severe water stress and underestimating the AGB, such as in the west of T1

Formatado: Inglês (Estados Unidos)

Excluído: Even though there is evidence that in the Amazonia-Cerrado transition the carbon allocation rates may vary in some situations of water stress, the INLAND model do not represent this strategy..

Formatado: Fonte: Não Negrito, Inglês (Estados Unidos)

Formatado: Inglês (Estados Unidos)

Formatado: Fonte: Não Negrito, Inglês (Estados Unidos)

Formatado: Inglês (Estados Unidos)

Formatado: Fonte: Não Negrito, Inglês (Estados Unidos)

595 T2, T3 and T4, located in the central part of the Amazon-Cerrado transition, showed the highest
596 average correlations between observed and simulated data (Table 7). For these transects, INLAND seems
597 to be able to capture the high variability of AGB gradient.

598 At T5, located at the south of the transition, the average correlations were low for all treatments,
599 indicating that INLAND has difficulty to represent the AGB gradient there (Table 7). However, it captures
600 the lower AGB as compared to the northern ones. In this region, the vegetation is characterized by a wide
601 diversity of physiognomies, which varies with other preponderant factors, such as lithology, soil depth,
602 topography and fertility. The observed data also showed high AGB variability, indicating that there are
603 changes in the vegetation structure, featuring medium-sized and small vegetation types on different soil
604 types. In INLAND, however, features such as lithology and water-table depth are not considered due to
605 the complexity of its representation on the large scale, limiting the representation of a heterogeneous
606 environment throughout the transition.

607 Patterns of vegetation distribution along the Amazon-Cerrado border exist are influenced not only
608 by inter-annual climate variability, P limitation, and fire, but also by the ecophysiological parameters.
609 Additional field experiments are needed to understand the relationship between currently fixed parameters
610 (such as carbon allocation, residence time, and deciduousness, among others) to the environmental
611 conditions and soil proprieties.

612 Another point to discuss is that the model simulates, in a few pixels in southeastern Cerrado, very
613 robust simulations of the presence of savanna and grassland even in the absence of fire (Figure 6A-F and
614 6a-f). This is, in our view, a result of the intense water and heat stress in this region. In the Brazilian
615 Cerrado, the high temperatures (> 35 °C) combined to the dry season duration (as long as 6 months with

little or no rain) exposes the vegetation to a severely stressed situation, so that a low biomass, low LAI vegetation may exist without the need of a frequent disturbance.

5 Conclusions

This is the first study that uses modeling to assess the influence of inter-annual climate variability, fire occurrence and phosphorus limitation to represent the Amazon-Cerrado border. This study shows that, although the model forced by a climatological database is able to simulate basic characteristics of the Amazon-Cerrado transition, the addition of factors such as inter-annual climate variability, phosphorus limitation and fire gradually improves simulated vegetation types. These effects are not homogeneous along the latitudinal/longitudinal gradient, which makes the adequate simulation of biomass challenging in some places along the transition. Based on the F-statistic in Tables 3, 4 and 5, this work shows that fire is in the main determinant factor of the changes in vegetation structure (LAI, AGB) along the transition. The nutrient limitation is second in magnitude, stronger than the effect of inter-annual climate variability.

Overall, although INLAND typically simulates more than 80% of the variability of biomass in the transition zone, in many places the biomass is clearly not well simulated. Situations for clearly wet or markedly dry climate conditions were well simulated, but the simulations are generally poor for transitional areas where the environment selected physiognomies that have an intermediate behavior, as is the case of the transitional forests in northern Tocantins and Mato Grosso.

There is evidence that the inclusion of spatially explicit parameters such as woody biomass residence time, maximum carboxylation capacity (V_{max}), and NPP allocation to wood may improve

Excluído: are

Excluído: s

Amazon rainforest AGB simulation by DGVMs (Castanho et al., 2013). However, in the transition, the lack of field parameters measured limits the inclusion of the variability of these biophysical parameters in DGVMs. Additional field work and compilation of existing ones are necessary to obtain physiological and structural parameters through the Amazon-Cerrado border to establish numerical relationships between soil, climate and vegetation. With the help of these data, dynamic vegetation models will be able to improve simulation of current patterns and future changes in vegetation considering climate change scenarios. In addition, it is also needed to include not only the spatial variability, but also temporal variability in physiological parameters of vegetation, allowing a more realistic simulation of the soil-climate-vegetation relationship. Finally, our results reinforce the importance and need of the DGVMs to incorporate the nutrient limitation and fire occurrence to simulate the Amazon-Cerrado border position.

Excluído: the vegetation

Excluído: correctly

Excluído: simulate

6 Acknowledgements

We gratefully thank the Brazilian agencies FAPEMIG and CAPES for their financial support. Atul K Jain is funded by the U.S. National Science Foundation (NSF-AGS- 12-43071).

7 References

Andreoli, R. V., Ferreira de Souza, R. A., Kayano, M. T. and Candido, L. A.: Seasonal anomalous rainfall in the central and eastern Amazon and associated anomalous oceanic and atmospheric patterns, Int. J. Climatol., 32(8), 1193–1205, doi:10.1002/joc.2345, 2012.

Aragão, L. E. O. C., Malhi, Y., Metcalfe, D. B., Silva-Espejo, J. E., Jiménez, E., Navarrete, D., Almeida, S., Costa, A. C. L., Salinas, N., Phillips, O. L., Anderson, L. O., Baker, T. R., Goncalvez, P. H., Huamán-Ovalle, J., Mamani-Solórzano, M., Meir, P., Monteagudo, A., Peñuela, M. C., Prieto, A.,

663 Quesada, C. A., Rozas-Dávila, A., Rudas, A., Silva Junior, J. A. and Vásquez, R.: Above- and below-
664 ground net primary productivity across ten Amazonian forests on contrasting soils, Biogeosciences, 6,
665 2441–2488, doi:10.5194/bgd-6-2441-2009, 2009.
666 Arora, V. K. and Boer, G. J.: Fire as an interactive component of dynamic vegetation models, J.
667 Geophys. Res, 110, doi:10.1029/2005JG000042, 2005
668 Balch, J. K., Brando, P. M., Nepstad, D. C., Coe, M. T., Silvério, D., Massad, T. J., Davidson, E.
669 A., Lefebvre, P., Oliveira-Santos, C., Rocha, W., Cury, R. T. S., Parsons, A. and Carvalho, K. S.: The
670 Susceptibility of Southeastern Amazon Forests to Fire: Insights from a Large-Scale Burn Experiment,
671 Bioscience, 65(9), 893–905, doi:10.1093/biosci/biv106, 2015.
672 Beguería, S., Vicente-Serrano, S. M., Tomás-Burguera, M. and Maneta, M.: Bias in the variance
673 of gridded data sets leads to misleading conclusions about changes in climate variability. Int. J. Climatol.,
674 36: 3413–3422. doi:10.1002/joc.4561, 2016.
675 Betts, R. A., Cox, P. M., Collins, M., Harris, P. P., Huntingford, C. and Jones, C. D.: The role of
676 ecosystem-atmosphere interactions in simulated Amazonian precipitation decrease and forest dieback
677 under global climate warming, Theor. Appl. Climatol., 78, 157–175, doi:10.1007/s00704-004-0050-y,
678 2004.
679 Bonan, G. B.: Forests and climate change: forcings, feedbacks, and the climate benefits of forests,
680 Science, 320(5882), 1444–1449, doi:10.1126/science.1155121, 2008.
681 Bond, W. J., Woodward, F. I. and Midgley, G. F.: The global distribution of ecosystems in a world
682 without fire, New Phytol., 165(2), 525–538, doi:10.1111/j.1469-8137.2004.01252.x, 2005.

683 Botta, A. and Foley, J. A.: Effects of climate variability and disturbances on the Amazonian
684 terrestrial ecosystems dynamics, Global Biogeochem. Cycles, 16(4), doi:10.1029/2000GB001338, 2002.
685 Brando, P. M., Nepstad, D. C., Davidson, E. A., Trumbore, S. E., Ray, D. and Camargo, P.:
686 Drought effects on litterfall, wood production and belowground carbon cycling in an Amazon forest:
687 results of a throughfall reduction experiment, Philos. Trans. R. Soc. Lond. B. Biol. Sci., 363(1498), 1839–
688 48, doi:10.1098/rstb.2007.0031, 2008.
689 Castanho, A. D. A., Coe, M. T., Costa, M. H., Malhi, Y., Galbraith, D. and Quesada, C. A.:
690 Improving simulated Amazon forest AGB and productivity by including spatial variation in biophysical
691 parameters, Biogeosciences, 10(4), 2255–2272, doi:10.5194/bg-10-2255-2013, 2013.
692 Couto-Santos, F. R., Luizão, F. J. and Carneiro Filho, A.: The influence of the conservation status
693 and changes in the rainfall regime on forest-savanna mosaic dynamics in Northern Brazilian Amazonia,
694 Acta Amaz., 44(2), 197–206, 2014.
695 Cox, P. M., Betts, R. A., Jones, C. D., Spall, S. A. and Totterdell, I. J.: Acceleration of global
696 warming due to carbon-cycle feedbacks in a coupled climate model, Nature, 408(November), 184–187,
697 doi:10.1038/35041539, 2000.
698 Cox, P. M., Betts, R. A., Collins, M., Harris, P. P., Huntingford, C. and Jones, C. D.: Amazonian
699 forest dieback under climate-carbon cycle projections for the 21st century, Theor. Appl. Climatol., 78,
700 137–156, doi:10.1007/s00704-004-0049-4, 2004.
701 Dajoz, R.: Princípios de ecologia, 7º edição, Artmed, Porto Alegre, RS, Brazil 519pp, 2005.
702 Dantas, V. L., Batalha, M. A. and Pausas, J. G.: Fire drives functional thresholds on the savanna-
703 forest transition, Ecology, 94(11), 2454–2463, doi:10.1890/12-1629.1, 2013.

Davidson, E. A., Carvalho, C. J.R., Vieira, I. C. G., Figueiredo, R. D. O., Moutinho, P., Ishida, F.Y., Santos, M. T.P., Guerrero, J.B., Kalif, K. and Sabá, R.T.: Nitrogen and Phosphorus Limitation of Biomass Growth in a Tropical Secondary Forest, Ecol. Appl., 14(4), 150–163, doi:10.1890/01-6006, 2004.

Dias, L. C. P., Macedo, M. N., Costa, M. H., Coe, M. T. and Neill, C.: Effects of land cover change on evapotranspiration and streamflow of small catchments in the Upper Xingu River Basin, Central Brazil, J. Hydrol. Reg. Stud., 4, 108–122, doi:10.1016/j.ejrh.2015.05.010, 2015.

Elias, F., Marimon, B. S., Matias, S. R. A., Forsthofer, M., Morandi, P. S. and Marimon-junior, B. H.: Dinâmica da distribuição espacial de populações arbóreas, ao longo de uma década, em cerradão na transição Cerrado-Amazônia, Mato Grosso, Biota Amaz., 3, 1–14, 2013.

Favier, C., Chave, J., Fabing, A., Schwartz, D. and Dubois, M. A.: Modelling forest-savanna mosaic dynamics in man-influenced environments: Effects of fire, climate and soil heterogeneity, Ecol. Modell., 171, 85–102, doi:10.1016/j.ecolmodel.2003.07.003, 2004.

Foley, J. A., Prentice, I. C., Ramankutty, N., Levis, S., Pollard, D., Sitch, S. and Haxeltine, A.: An integrated biosphere model of land surface processes, terrestrial carbon balance, and vegetation dynamics, Global Biogeochem. Cycles, 10, 603, doi:10.1029/96GB02692, 1996.

Foley, J. A., Botta,A., Coe, M. T. and Costa, M. H.: El Niño–Southern oscillation and the climate, ecosystems and rivers of Amazonia, Global Biogeochem. Cycles, 16(4), 1132, doi:10.1029/2002GB001872, 2002.

Goedert, W: Solos do Cerrado: Tecnologias e Estratégias de Manejo, Empresa Brasileira de Pesquisa Agropecuária (EMBRAPA), Brasília, DF, Brasil. 422pp., 1986.

Goll, D. S., V. Brovkin, B. R. Parida, C. H. Reick, J. Kattge, P. B. Reich, P. M. Van Bodegom, and Ü. Niinemets.: Nutrient limitation reduces land carbon uptake in simulations with a model of combined carbon, nitrogen and phosphorus cycling, Biogeosciences, 9(C), 3547–3569, doi:10.5194/bg-9-3547-2012,2012.

Hansen, M. C. and Reed, B.: A comparison of the IGBP DISCover and University of Maryland 1km global land cover products, Int. J. Remote Sens., 21, 1365–1373, doi:10.1080/014311600210218, 2000.

Harris, I., Jones, P. D., Osborn, T. J. and Lister, D. H.: Updated high-resolution grids of monthly climatic observations - the CRU TS3.10 Dataset, Int. J. Climatol., 34(3), 623–642, doi:10.1002/joc.3711, 2014.

Hilker, T., Lyapustin, A. I., Tucker, C. J., Hall, F. G., Myneni, R. B., Wang, Y., Bi, J., Mendes de Moura, Y. and Sellers, P. J.: Vegetation dynamics and rainfall sensitivity of the Amazon., Proc. Natl. Acad. Sci. U. S. A., 111(45), 16041–6, doi:10.1073/pnas.1404870111, 2014.

Hirota, M., Nobre, C., Oyama, M. D. and Bustamante, M. M. C.: The climatic sensitivity of the forest, savanna and forest-savanna transition in tropical South America, New Phytol., 187, 707–719, doi:10.1111/j.1469-8137.2010.03352.x, 2010.

Hoffmann, W. A., B. Orthen, and P. K. V. Nascimento.: Comparative fire ecology of tropical savanna and forest trees, Functional Ecology, 17:720–726, 2003.

Hoffmann, W.A., Adasme, R., Haridasan, M., Carvalho, M., Geiger, E.L., Pereira, M.A.B., Gotsch, S.G., and Franco, A.C.:Tree topkill, not mortality, governs the dynamics of alternate stable states at savanna-forest boundaries under frequent fire in central Brazil, Ecology, 90, 1326–1337, 2009.

Formatado: Justificado, Recuo: Primeira linha: 1,25 cm, Espaço Depois de: 0 pt, Espaçamento entre linhas: Duplo

Formatado: Inglês (Estados Unidos)

Excluído: ¶

747 Hoffmann, W. A., Geiger, E. L., Gotsch, S. G., Rossatto, D. R., Silva, L. C. R., Lau, O. L.,
748 Haridasan, M. and Franco, A. C.: Ecological thresholds at the savanna-forest boundary: How plant traits,
749 resources and fire govern the distribution of tropical biomes, Ecol. Lett., 15, 759–768,
750 doi:10.1111/j.1461-0248.2012.01789.x, 2012.
751 House, J. I., Archer, S., Breshears, D. D. and Scholes, R. J.: Conundrums in mixed woody-
752 herbaceous plant systems, J. Biogeogr., 30, 1763–1777, doi:10.1046/j.1365-2699.2003.00873.x, 2003.
753 IBGE.: Manual Técnico da Vegetação Brasileira (Manuais Técnicos em Geociências n. 1),
754 Fundação Instituto Brasileiro de Geografia e Estatística (IBGE), Rio de Janeiro, RJ, Brasil. 92pp., 1992.
755 IBGE.: Mapa da Vegetação do Brasil, Fundação Instituto Brasileiro de Geografia e Estatística
756 (IBGE), Rio de Janeiro, RJ, Brazil, Map, 2004.
757 Klink, C. A. and Machado, R. B.: Conservation of the Brazilian Cerrado, Conserv. Biol., 19(3),
758 707–713, doi:10.1111/j.1523-1739.2005.00702.x, 2005.
759 Kucharik, C. J., Foley, J. A., Delire, C., Fisher, V. A., Coe, M. T., Lenters, J. D., Young-Molling,
760 C., Ramankutty, N., Norman, J. M. and Gower, S. T.: Testing the performance of a Dynamic Global
761 Ecosystem Model: Water balance, carbon balance, and vegetation structure, Global Biogeochem. Cycles,
762 14(3), 795–825, doi:10.1029/1999GB001138, 2000.
763 Lee, J. E., Frankenberg, C., van der Tol, C., Berry, J. A., Guanter, L., Boyce, C. K., Fisher, J. B.,
764 Morrow, E., Worden, J. R., Asefi, S., Badgley, G. and Saatchi, S.: Forest productivity and water stress in
765 Amazonia: observations from GOSAT chlorophyll fluorescence, Proc. R. Soc. B Biol. Sci., 280(1761),
766 20130171–20130171, doi:10.1098/rspb.2013.0171, 2013.

767 Lehmann, C. E. R., Archibald, S. A., Hoffmann, W. A. and Bond, W. J.: Deciphering the
768 distribution of the savanna biome, New Phytol., 191, 197–209, doi:10.1111/j.1469-8137.2011.03689.x,
769 2011.
770 Lehmann, C. E. R., Anderson, T. M., Sankaran, M., Higgins, S. I., Archibald, S., Hoffmann, W.
771 A., Hanan, N. P., Williams, R. J., Fensham, R. J., Felfili, J., Hutley, L. B., Ratnam, J., Jose, J. S., Montes,
772 R., Franklin, D., Russell-Smith, J., Ryan, C. M., Durigan, G., Hiernaux, P., Haidar, R., Bowman, D. M.
773 J. S., and Bond, W. J.: Savanna Vegetation-Fire-Climate Relationships Differ Among Continents,
774 Science, 343 (January), 548–553, doi:10.1126/science.1247355, 2014.
775 Long, W., Yang, X. and Donghai, L.: Patterns of species diversity and soil nutrients along a
776 chronosequence of vegetation recovery in Hainan Island, South China, Ecol. Res., 2012.
777 Malhi, Y., Aragão, L. E. O. C., Metcalfe, D. B., Paiva, R., Quesada, C. A., Almeida, S., Anderson,
778 L., Brando, P., Chambers, J. Q., da Costa, A. C. L., Hutyra, L. R., Oliveira, P., Patiño, S., Pyle, E. H.,
779 Robertson, A. L. and Teixeira, L. M.: Comprehensive assessment of carbon productivity, allocation and
780 storage in three Amazonian forests, Glob. Chang. Biol., 15, 1255–1274, doi:10.1111/j.1365-
781 2486.2008.01780.x, 2009.
782 Marengo, J. A.: Interdecadal variability and trends of rainfall across the Amazon basin, Theor.
783 Appl. Climatol., 78(1–3), 79–96, doi:10.1007/s00704-004-0045-8, 2004.
784 Marimon Junior, B. H. and Haridasan, M.: Comparação da vegetação arbórea e características
785 edáficas de um cerradão e um cerrado sensu stricto em áreas adjacentes sobre solo distrófico no leste de
786 Mato Grosso, Brasil, Acta Bot. Brasilica, 19(4), 913–926, doi:10.1590/S0102-33062005000400026,
787 2005.

Marimon, B. S., Lima, E. S., Duarte, T. G., Chieregatto, L. C., Ratter, J. A.: Observations on the vegetation of northeastern Mato Grosso, Brazil. IV. An analysis of the Cerrado-Amazonian Forest ecotone, Edinburgh Journal of Botany, 63, 323–341, doi: 10.1017/S0960428606000576, 2006.

Marimon, B. S., Marimon-Junior, B. H., Feldpausch, T. R., Oliveira-Santos, C., Mews, H. A., Lopez-Gonzalez, G., Lloyd, J., Franczak, D. D., de Oliveira, E. A., Maracahipes, L., Miguel, A., Lenza, E. and Phillips, O. L.: Disequilibrium and hyperdynamic tree turnover at the forest–cerrado transition zone in southern Amazonia, Plant Ecol. Divers., 7(1–2), 281–292, doi:10.1080/17550874.2013.818072, 2014.

Mercado, L. M., Patino, S., Domingues, T. F., Fyllas, N. M., Weedon, G. P., Sitch, S., Quesada, C. A., Phillips, O. L., Aragao, L. E. O. C., Malhi, Y., Dolman, A. J., Restrepo-Coupe, N., Saleska, S. R., Baker, T. R., Almeida, S., Higuchi, N. and Lloyd, J.: Variations in Amazon forest productivity correlated with foliar nutrients and modelled rates of photosynthetic carbon supply, Philos. Trans. R. Soc. Lond. B. Biol. Sci., 366(1582), 3316–3329, doi:10.1098/rstb.2011.0045, 2011.

Morandi, P.S., Marimon-Junior, B. H., Oliveira, E. A., Reis, S. M. A., Valadão, M. B. X., Forsthofer, M., Passos, F. B., Marimon, B. S.: Vegetation Succession in the Cerrado-Amazonian Forest Transition Zone of Mato Gross State, Brazil, Edinburgh Journal of Botany, 73, 83-93, doi: 10.1017/S096042861500027X, 2016.

Moreno, M. I. C., Schiavini, I. and Haridasan, M.: Fatores edáficos influenciando na estrutura de fitofisionomias do cerrado, Caminhos da Geogr., 9(25), 173–194, 2008.

Murphy, B. P. and Bowman, D. M. J. S.: What controls the distribution of tropical forest and savanna?, Ecol. Lett., 15, 748–758, doi:10.1111/j.1461-0248.2012.01771.x, 2012.

Myers, N., Fonseca, G. A B., Mittermeier, R. A, Fonseca, G. A. B. and Kent, J.: Biodiversity hotspots for conservation priorities, Nature, 403(6772), 853–858, doi:10.1038/35002501, 2000.

Nardoto, G. B., Bustamante, M. M. C., Pinto, A. S. and Klink, C. A. Nutrient use efficiency at ecosystem and species level in savanna areas of Central Brazil and impacts of fire, J. Trop. Ecol., 22, 191–201, doi:10.1017/S0266467405002865, 2006.

Nogueira, E. M., Yanai, A. M., Fonseca, F. O. and Fearnside, P. M.: Carbon stock loss from deforestation through 2013 in Brazilian Amazonia, Glob. Chang. Biol., doi:10.1111/gcb.12798, 2015.

Nunes, E. L., Costa, M. H., Malhado, A. C. M., Dias, L. C. P., Vieira, S. A., Pinto, L. B. and Ladle, R. J.: Monitoring carbon assimilation in South America's tropical forests: Model specification and application to the Amazonian droughts of 2005 and 2010, Remote Sens. Environ., 117, 449–463, doi:10.1016/j.rse.2011.10.022, 2012.

Oliveira, B., Marimon-Junior, B. H., Mews, H. A., Valadão, M. B. X., Marimon, B. S.: Unraveling the ecosystem functions in the Amazonia–Cerrado transition: evidence of hyperdynamic nutrient cycling, Plant Ecol., 218(2), 225–239, doi:10.1007/s11258-016-0681-y, 2017.

Oyama, M. D. and Nobre, C. A.: A new climate-vegetation equilibrium state for Tropical South America, Geophys. Res. Lett., 30(23), 10–13, doi:10.1029/2003GL018600, 2003.

Parton, W. J., Scurlock, J. M. O., Ojima, D. S., Gilmanov, T. G., Scholes, R. J., Schimel, D. S., Kirchner, T., Menaut, J.-C., Seastedt, T., Garcia Moya, E., Kamnalrut, A. and Kinyamario, J. I.: Observations and modeling of AGB and soil organic matter dynamics for the grassland biome worldwide, Global Biogeochem. Cycles, 7, 785, doi:10.1029/93GB02042, 1993.

Pereira, M. P. S., Malhado, A. C. M. and Costa, M. H.: Predicting land cover changes in the Amazon rainforest: An ocean-atmosphere-biosphere problem, Geophys. Res. Lett., 39(9), doi:10.1029/2012GL051556, 2012.

Pires, G. F. and Costa, M. H.: Deforestation causes different subregional effects on the Amazon bioclimatic equilibrium, Geophys. Res. Lett., 40(14), 3618–3623, doi:10.1002/grl.50570, 2013.

Quesada, C. A., Lloyd, J., Schwarz, M., Baker, T. R., Phillips, O. L., Patiño, S., Czimczik, C., Hodnett, M. G., Herrera, R., Arneth, A., Lloyd, G., Malhi, Y., Dezzeo, N., Luizão, F. J., Santos, A. J. B., Schmerler, J., Arroyo, L., Silveira, M., Priante Filho, N., Jimenez, E. M., Paiva, R., Vieira, I., Neill, D. A., Silva, N., Peñuela, M. C., Monteagudo, A., Vásquez, R., Prieto, A., Rudas, A., Almeida, S., Higuchi, N., Lezama, A. T., López-González, G., Peacock, J., Fyllas, N. M., Alvarez Dávila, E., Erwin, T., di Fiore, A., Chao, K. J., Honorio, E., Killeen, T., Peña Cruz, A., Pitman, N., Núñez Vargas, P., Salomão, R., Terborgh, J. and Ramírez, H.: Regional and large-scale patterns in Amazon forest structure and function are mediated by variations in soil physical and chemical properties, Biogeosciences Discuss., 6, 3993–4057, doi:10.5194/bgd-6-3993-2009, 2009.

Quesada, C. A., Lloyd, J., Anderson, L. O., Fyllas, N. M., Schwarz, M. and Czimczik, C. I.: Soils of Amazonia with particular reference to the RAINFOR sites, Biogeosciences, 8, 1415–1440, doi:10.5194/bg-8-1415-2011, 2011.

Quesada, C. A., Phillips, O. L., Schwarz, M., Czimczik, C. I., Baker, T. R., Patiño, S., Fyllas, N. M., Hodnett, M. G., Herrera, R., Almeida, S., Alvarez Dávila, E., Arneth, A., Arroyo, L., Chao, K. J., Dezzeo, N., Erwin, T., Di Fiore, A., Higuchi, N., Honorio Coronado, E., Jimenez, E. M., Killeen, T., Lezama, A. T., Lloyd, G., Löpez-González, G., Luizão, F. J., Malhi, Y., Monteagudo, A., Neill, D. A.,

Núñez Vargas, P., Paiva, R., Peacock, J., Peñuela, M. C., Peña Cruz, A., Pitman, N., Priante Filho, N., Prieto, A., Ramírez, H., Rudas, A., Salomão, R., Santos, A. J. B., Schmerler, J., Silva, N., Silveira, M., Vásquez, R., Vieira, I., Terborgh, J. and Lloyd, J.: Basin-wide variations in Amazon forest structure and function are mediated by both soils and climate, Biogeosciences, 9(6), 2203–2246, doi:10.5194/bg-9-2203-2012, 2012.

Reis, S. M., Marimon, B. S., Marimon Junior, B.-H., Gomes, L., Morandi, P. S., Freire, E. G. and Lenza, E.: Resilience of savanna forest after clear-cutting in the Cerrado-Amazon transition zone, Bioscience, 31(5), 1519–1529, doi:10.14393/BJ-v31n5a2015-26368, 2015.

Restrepo-Coupe, N., da Rocha, H. R., Hutyra, L. R., da Araujo, A. C., Borma, L. S., Christoffersen, B., Cabral, O. M. R., de Camargo, P. B., Cardoso, F. L., da Costa, A. C. L., Fitzjarrald, D. R., Goulden, M. L., Kruijt, B., Maia, J. M. F., Malhi, Y. S., Manzi, A. O., Miller, S. D., Nobre, A. D., von Randow, C., S, L. D. A., Sakai, R. K., Tota, J., Wofsy, S. C., Zanchi, F. B. and Saleska, S. R.: What drives the seasonality of photosynthesis across the Amazon basin? A cross-site analysis of eddy flux tower measurements from the Brazil flux network, Agric. For. Meteorol., 182–183, 128–144, doi:10.1016/j.agrformet.2013.04.031, 2013.

Rezende, A. V, Sanquetta, C. R. and Filho, F. A.: Efeito do desmatamento no estabelecimento de espécies lenhosas em um cerrado Sensu stricto, Floresta, 35, 69–88, 2005.

Ribeiro, J. F. and Walter, B. M. T.: As Principais Fitofisionomias do bioma Cerrado, in Cerrado: ecologia e flora, pp. 153–212., 2008.

869 Rocha, H. R. da, Goulden, M. L., Miller, S. D., Menton, M. C., Pinto, L. D. V. O., De Freitas, H.
870 C. and Figueira, A. M. E. S.: Seasonality of water and heat fluxes over a tropical forest in eastern
871 Amazonia, Ecol. Appl., 14(4 SUPPL.), doi:10.1890/02-6001, 2004.
872 Roy, S. B. and Avissar, R.: Impact of land use/land cover change on regional hydrometeorology
873 in Amazonia, J. Geophys. Res., 107(D20), 1–12, doi:10.1029/2000JD000266, 2002.
874 Saatchi, S., Houghton, R. A., Dos Santos Alvalá, R. C., Soares, J. V. and Yu, Y.: Distribution of
875 aboveground live AGB in the Amazon basin, Glob. Chang. Biol., 13(4), 816–837, doi:10.1111/j.1365-
876 2486.2007.01323.x, 2007.
877 Salazar, L. F., Nobre, C. A. and Oyama, M. D.: Climate change consequences on the biome
878 distribution in tropical South America, Geophys. Res. Lett., 34(April), 2–7, doi:10.1029/2007GL029695,
879 2007.
880 Senna, M. C. A., Costa, M. H., Pinto, L. I.C., Imbuzeiro, H. M. A., Diniz, L. M. F. and Pires, G.
881 F.: Challenges to reproduce vegetation structure and dynamics in Amazonia using a coupled climate-
882 biosphere model, Earth Interact., 13(11), doi:10.1175/2009EI281.1, 2009.
883 Shukla, J., Nobre, C. and Sellers, P.: Amazon deforestation and climate change, Science, 247,
884 1322–1325, doi:10.1126/science.247.4948.1322, 1990.
885 Silva, J. F., Fariñas, M. R., Felfili, J. M. and Klink, C. A.: Spatial heterogeneity, land use and
886 conservation in the cerrado region of Brazil, in Journal of Biogeography, vol. 33, pp. 536–548., 2006.
887 Silvério, D. V, Brando, P. M., Balch, J. K., Putz, F. E., Nepstad, D. C., Oliveira-Santos, C. and
888 Bustamante, M. M. C.: Testing the Amazon savannization hypothesis: fire effects on invasion of a

889 neotropical forest by native cerrado and exotic pasture grasses, Philos. Trans. R. Soc. Lond. B. Biol. Sci.,
890 368, 20120427, doi:10.1098/rstb.2012.0427, 2013.
891 Smith, B., Wärlind, D., Arneth, A., Hickler, T., Leadley, P., Siltberg, J. and Zaehle, S.:
892 Implications of incorporating N cycling and N limitations on primary production in an individual-based
893 dynamic vegetation model, Biogeosciences, 11(7), 2027–2054, doi:10.5194/bg-11-2027-2014, 2014.
894 Thompson, S. L. and Pollard, D.: A global climate model (GENESIS) with a land-surface transfer
895 scheme (LSX). Part I: present climate simulation, J. Clim., 8, 732–761, doi:10.1175/1520-
896 0442(1995)008<0732:AGCMWA>2.0.CO;2, 1995.
897 Torello-Raventos, M., Feldpausch, T., Veenendaal, E., Schrodt, F., Saiz, G., Domingues, T.,
898 Djagbletey, G., Ford, A., Kemp, J., Marimon, B., Hur Marimon Junior, B., Lenza, E., Ratter, J.,
899 Maracahipes, L., Sasaki, D., Sonké, B., Zapfack, L., Taedoumg, H., Villarroel, D., Schwarz, M., Quesada,
900 C., Yoko Ishida, F., Nardoto, G., Affum-Baffoe, K., Arroyo, L., Bowman, D., Compaore, H., Davies, K.,
901 Diallo, A., Fyllas, N., Gilpin, M., Hien, F., Johnson, M., Killeen, T., Metcalfe, D., Miranda, H., Steininger,
902 M., Thomson, J., Sykora, K., Mougin, E., Hiernaux, P., Bird, M., Grace, J., Lewis, S., Phillips, O. and
903 Lloyd, J.: On the delineation of tropical vegetation types with an emphasis on forest/savanna transitions,
904 Plant Ecol. Divers., 6, 101–137, doi:10.1080/17550874.2012.76281, 2013.
905 Valadão, M. B. X., Marimon-Junior, B. H., Oliveira, B., Lúcio, N. W., Souza, M. G. R., Marimon,
906 B. S.: AGB hyperdynamic as a key modulator of forest self-maintenance in dystrophic soil at Amazonia-
907 Cerrado transition. Scientia Forestalis, 44, 475-485, 2016.
908 Veenendaal, E. M., Torello-Raventos, M., Feldpausch, T. R., Domingues, T. F., Gerard, F.,
909 Schrodt, F., Saiz, G., Quesada, C. A., Djagbletey, G., Ford, A., Kemp, J., Marimon, B. S., Marimon-

910 Junior, B. H., Lenza, E., Ratter, J. A., Maracahipes, L., Sasaki, D., Sonk, B., Zapfack, L., Villarroel, D.,
911 Schwarz, M., Yoko Ishida, F., Gilpin, M., Nardoto, G. B., Affum-Baffoe, K., Arroyo, L., Bloomfield, K.,
912 Ceca, G., Compaore, H., Davies, K., Diallo, A., Fyllas, N. M., Gignoux, J., Hien, F., Johnson, M., Mougin,
913 E., Hiernaux, P., Killeen, T., Metcalfe, D., Miranda, H. S., Steininger, M., Sykora, K., Bird, M. I., Grace,
914 J., Lewis, S., Phillips, O. L. and Lloyd, J.: Structural, physiognomic and above-ground AGB variation in
915 savanna-forest transition zones on three continents - How different are co-occurring savanna and forest
916 formations?, Biogeosciences, 12(10), 2927–2951, doi:10.5194/bg-12-2927-2015, 2015.

917 Verberne, E. L. J., Hassink, J., De Willigen, P., Groot, J. J. R. and Van Veen, J. A.: Modelling
918 organic matter dynamics in different soils, Netherlands J. Agric. Sci., 38, 221–238, 1990.

919 Vourlitis, G. L., de Lobo, F. A., Lawrence, S., de Lucena, I. C., Pinto, O. B., Dalmagro, H. J.,
920 Ortiz, C. E. and de Nogueira, J. S.: Variations in Stand Structure and Diversity along a Soil Fertility
921 Gradient in a Brazilian Savanna (Cerrado) in Southern Mato Grosso, Soil Sci. Soc. Am. J., 77(4), 1370–
922 1379, doi:10.2136/sssaj2012.0336, 2013.

923 Wang, S., Huang, J., He, Y. and Guan, Y.: Combined effects of the Pacific Decadal Oscillation
924 and El Niño-Southern Oscillation on Global Land Dry–Wet Changes, Sci. Rep., 4, 6651,
925 doi:10.1038/srep06651, 2014.

926 Yang, X. and Post, W. M.: Phosphorus transformations as a function of pedogenesis: A synthesis
927 of soil phosphorus data using Hedley fractionation method, Biogeosciences, 8, 2907–2916,
928 doi:10.5194/bg-8-2907-2011, 2011.

929 Yang, X., Post, W. M., Thornton, P. E. and Jain, A.: The distribution of soil phosphorus for global
930 biogeochemical modeling, Biogeosciences, 10, 2525–2537, doi:10.5194/bg-10-2525-2013, 2013.

Formatado: Inglês (Estados Unidos)

931 Yang, X., Thornton, P. E., Ricciuto, D. M. and Post, W. M.: The role of phosphorus dynamics in
932 tropical forests - A modeling study using CLM-CNP, Biogeosciences, 11, 1667–1681, doi:10.5194/bg-
933 11-1667-2014, 2014.
934
935

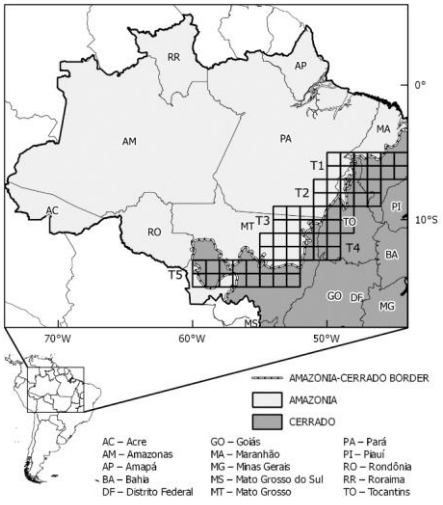

Figure 1. Delimitation of the study area Amazonia (in light gray) and Cerrado (in dark gray) (IBGE, 2004), and the location of five transects used in this work (from T1 to T5). The dashed line represents the border between biomes.

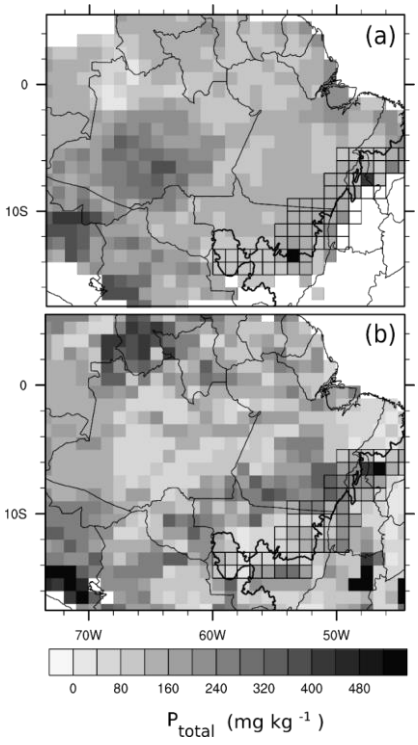

Figure 2. (a) Map of regional total P in the soil (PR), (b) Map of global total P in the soil (Yang et al., 2013) (PG).

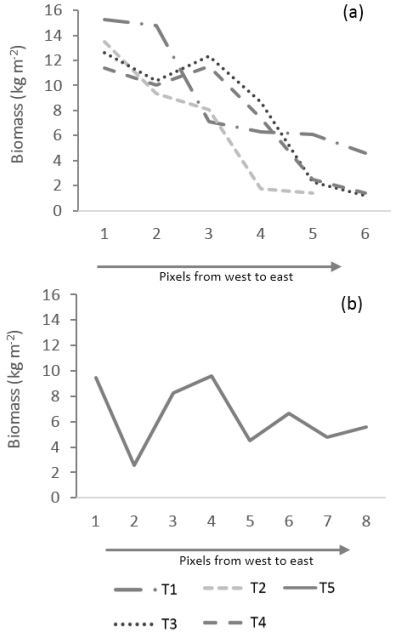

944

945 **Figure 3.** Average variations of AGB in pixels from West to East in the Amazonia-Cerrado transition

946 for transects T1, T2, T3 and T4 (a), and T5 (b).

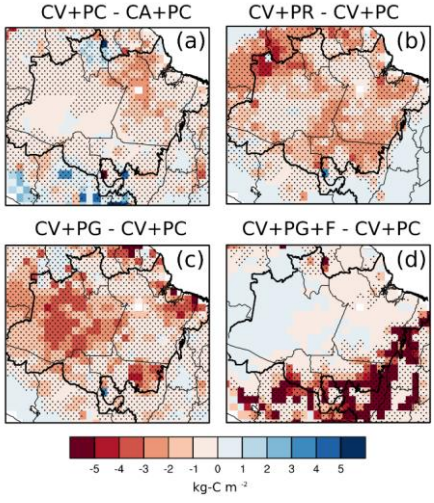

Figure 4. Effects of inter-annual climate variability (a), Regional P limitation (b), Global P limitation (c), and fire (d) on AGB. The hatched areas indicate that the variables are significantly different compared to the control simulation at the level of 95% according to the t-test. The thick black line is the geographical limits of the biomes.

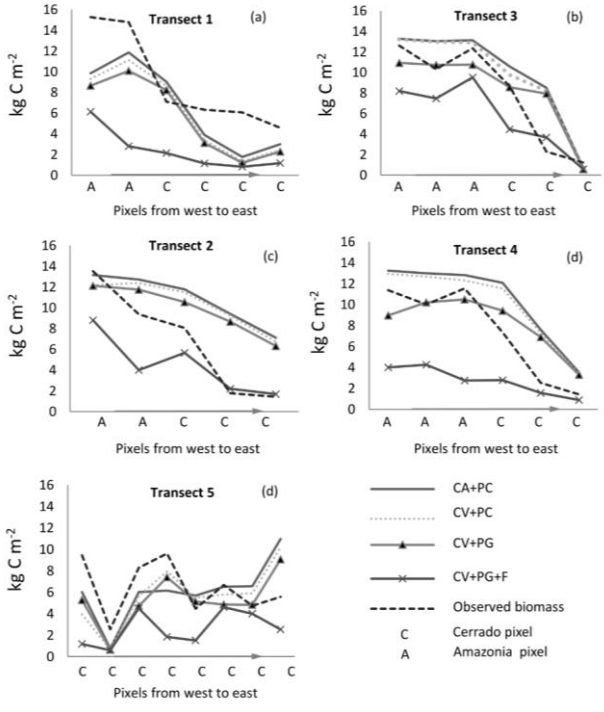

952

953 **Figure 5.** Average longitudinal AGB gradient in Amazonia-Cerrado transition simulated for T1 to T5
954 considering different combinations: observed data; seasonal climate control simulation (CA+PC); inter-
955 annual climate variability (CV+PC); inter-annual climate variability + global P limitation (CV+PG); and
956 inter-annual climate variability + P + fire occurrence (CV+PG+F).

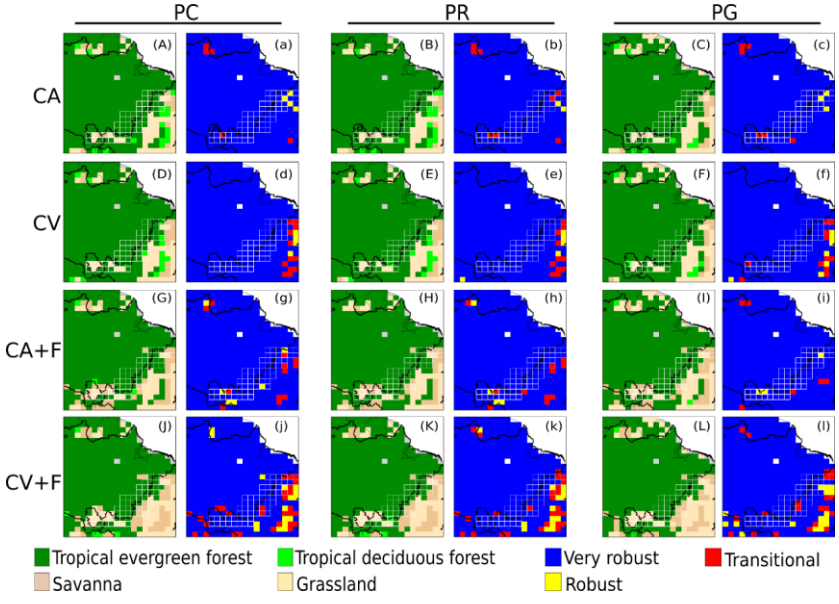

Figure 6. Results for the dominant vegetation cover simulated by INLAND for the different treatments (A-L) and a metric of variability of results (a-l). Simulations are considered very robust if the dominant vegetation agrees on 9-10 of the last 10 years of simulation, robust if it agrees on 7-8 years, and transitional if on 6 or fewer years.

Table 1. Simulations with different scenarios evaluated by INLAND model in Amazonia-Cerrado transition. CA, climatological average, 1961-1990; CV, monthly climate data, 1948-2008; the nutrient limitation on V_{max} - PC, no P limitation (V_{max} = 65 μmol-CO_2 m^{-2} s^{-1}); PR, regional P limitation; PG, global P limitation).

			V_{max}		
Climate	**CO_2**	**Fire (F)**	**PC**	**PR**	**PG**
CA	Variable	Off	CA+PC	CA+PR	CA+PG
CA	Variable	On	CA+PC+F	CA+PR+F	CA+PG+F
CV	Variable	Off	CV+PC	CV+PR	CV+PG
CV	Variable	On	CV+PC+F	CV+PR+F	CV+PG+F

971 **Table 2.** Individual and combined effects for each simulation in Amazonia-Cerrado transition. CA,
972 climatological seasonal average, 1961-1990; CV, monthly climate data, 1948-2008; the nutrient limitation
973 on V_{max} - PC, no P limitation (V_{max} = 65 μmolCO_2 m^{-2} s^{-1}); PR, regional P limitation; PG, global P
974 limitation)

Climate (C)	Phosphorus (P)	Fire (F)
(CV+PC)-(CA+PC)	(CA+PR)-(CA+PC)	(CA+PC+F)-(CA+PC)
(CV+PR)-(CA+PR)	(CV+PR)-(CV+PC)	(CV+PC+F)-(CV+PC)
(CV+PG)-(CA+PG)	(CA+PG)-(CA+PC)	(CA+PR+F)-(CA+PR)
	(CV+PG)-(CV+PC)	(CV+PR+F)-(CV+PR)
		(CA+PG+F)-(CA+PG)
		(CV+PG+F)-(CV+PG)

975
976

977 **Table 3.** Summary of average NPP, LAI and AGB for the Amazonia-Cerrado transition at the transects
978 domains, considering all simulations with CA and CV regardless of fire presence or P limitation. The
979 results of a one-way ANOVA are also shown, including the *F* statistic, and p value. Values within each
980 column followed by a different letter are significantly different ($p < 0.05$) according to the Tukey–Kramer
981 test (n=1860: 31 pixels x 10 years x $n_{simulation/2}$).

Group 1	**NPP**		**LAI_{total}**		**LAI_{lower}**		**LAI_{upper}**		**AGB**	
	kg-C m^{-2} yr^{-1}		m^2 m^{-2}		m^2 m^{-2}		m^2 m^{-2}		kg-C m^{-2}	
CA	0.68	a	7.47	a	1.98	a	5.49	a	6.68	a
CV	0.64	b	7.15	b	2.11	a	5.04	b	6.30	b
F	*40.2*		*57.2*		*2.96*		*36.0*		*11.3*	
p	*<0.001*		*<0.001*		*ns*		*<0.01*		*<0.001*	

982

983

Table 4. Summary of average NPP, LAI and AGB for the transition at the transects domains, considering different P limitation, regardless of climate and fire presence. The results of a one-way ANOVA are also shown, including the *F* statistic, and p value. Values within each column followed by a different letter are significantly different ($p < 0.05$) according to the Tukey–Kramer test (n=1240: 31 pixels x 10 years x $n_{simulation/3}$).

Group 2	**NPP**		**LAI_{total}**		**LAI_{lower}**		**LAI_{upper}**		**AGB**	
	kg-C m^{-2} yr^{-1}		m^2 m^{-2}		m^2 m^{-2}		m^2 m^{-2}		kg-C m^{-2}	
PC	0.71	a	7.64	a	1.84	b	5.80	a	7.15	a
PR	0.64	b	7.15	b	2.19	a	4.95	b	6.20	b
PG	0.64	b	7.14	b	2.10	a	5.04	b	6.12	b
$F_{2,99}$	*62.8*		*61.0*		*8.75*		*53.5*		*33.6*	
p	*<0.001*		*<0.001*		*<0.01*		*<0.01*		*<0.001*	

Table 5. Summary of average NPP, LAI and AGB for the transition at the transects domains, considering presence or absence of fire. The results of a one-way ANOVA are also shown, including the *F* statistic, and p value. Values within each column followed by a different letter are significantly different ($p < 0.05$) according to the Tukey–Kramer test (n=1860: 31 pixels x 10 years x $n_{simulation/2}$).

Group 3	**NPP**		**LAI_{total}**		**LAI_{lower}**		**LAI_{upper}**		**AGB**	
	kg-C m^{-2} yr^{-1}		m^2 m^{-2}		m^2 m^{-2}		m^2 m^{-2}		kg-C m^{-2}	
Fire OFF	0.66	a	6.72	b	0.88	b	5.84	a	8.47	b
Fire ON	0.67	b	7.90	a	3.21	a	4.69	b	4.51	a
$F_{3.84}$	*8.28*		*937*		1459		249		1719	
p	*<0.005*		*<0.001*		*<0.01*		*<0.01*		*<0.001*	

997 **Table 6.** Summary of average NPP, LAI and AGB for the transition at the transects domains, considering
998 all factor combinations. The results of a one-way ANOVA are also shown, including the *F* statistic, and
999 p value. Values within each column followed by a different letter are significantly different ($p < 0.05$)
1000 according to the Tukey–Kramer test (n=310: 31 pixels x 10 years).

	NPP		**LAI_{total}**		**LAI_{lower}**		**LAI_{upper}**		**AGB**	
	kg-C m^{-2} yr^{-1}		m^2 m^{-2}		m^2 m^{-2}		m^2 m^{-2}		kg-C m^{-2}	
CV+PC	0.69	bcd	6.96	d	0.84	e	6.48	a	9.01	ab
CV+PG	0.61	f	6.24	f	0.85	e	5.60	bc	7.91	c
CV+PR	0.62	f	6.33	f	0.85	e	5.74	bc	8.04	c
CV+PC+F	0.69	abc	7.92	b	2.91	cd	4.61	ef	4.89	de
CV+PG+F	0.63	ef	7.76	b	3.73	a	5.81	bc	3.91	f
CV+PR+F	0.63	ef	7.65	bc	3.47	ab	4.69	ef	4.02	f
CA+PC	0.72	ab	7.39	c	0.91	e	6.12	ab	9.31	a
CA+PG	0.64	def	6.64	e	0.91	e	5.40	cd	8.22	c
CA+PR	0.65	cdef	6.72	de	0.91	e	5.49	cd	8.31	bc
CA+PC+F	0.74	a	8.29	a	2.69	d	5.02	de	5.40	d
CA+PG+F	0.67	cde	7.90	b	3.29	abc	4.04	g	4.45	ef
CA+PR+F	0.67	cde	7.88	b	3.19	bc	4.18	fg	4.42	ef
F	*16.2*		*115*		*140*		38.1		*172*	
p	*<0.001*		*<0.001*		*<0.01*		*<0.01*		*<0.001*	

1001

1002 **Table 7**. Correlation coefficients of AGB simulated by INLAND and field estimates (n= 310: 31 pixels

1003 x 10 years).

	T1	T2	T3	T4	T5	All transects
CA+PC	0.843	0.928	0.886	0.937	0.337	0.786
CV+PC	0.838	0.884	0.890	0.939	0.355	0.781
CA+PR	0.793	0.848	0.830	0.911	0.399	0.756
CV+PR	0.795	0.793	0.832	0.907	0.527	0.771
CA+PG	0.814	0.951	0.838	0.889	0.388	0.776
CV+PG	0.825	0.922	0.840	0.879	0.496	0.792
CA+PC+F	0.988	0.987	0.977	0.892	0.133	0.795
CV+PC+F	0.976	0.947	0.933	0.908	0.187	0.790
CA+PR+F	0.842	0.805	0.981	0.808	0.561	0.799
CV+PR+F	0.925	0.804	0.927	0.808	0.319	0.757
CA+PG+F	0.844	0.961	0.980	0.830	0.430	0.809
CV+PG+F	0.845	0.932	0.931	0.881	0.177	0.753
CA avg	0.854	0.913	0.915	0.878	0.375	0.787
CV avg	0.867	0.880	0.892	0.887	0.344	0.774

1004